

# Computer model to investigate the effect of eye movements on retinal heating during long-duration fixation on a laser source

**Brian J. Lund**

Northrop Grumman IT  
4241 Woodcock Drive Suite B100  
San Antonio, Texas 78228  
E-mail: brian.lund@brooks.af.mil

**Abstract.** A computer simulation called RHME (Retinal Heating in Moving Eye) is developed to simulate the heating pattern that occurs in the retina during a long-duration exposure to a continuous wave laser beam. The simulation takes into account eye movements that occur during a deliberate fixation. Due to the rapid (millisecond) thermal time scale for heating and cooling, only the area of the retina directly exposed to the laser sustains an increased temperature. Once the laser spot is removed from a particular location of the retina (because of eye movements) that location quickly cools. Points of the retina will therefore have a complex thermal history during a long-duration exposure. Simulation results for a minimal retinal spot size indicate that subjects staring at a helium-neon laser ( $\lambda = 632.8$  nm) beam producing the small-source maximum permissible exposure (MPE) level corneal irradiance of  $1 \text{ mW cm}^{-2}$  ( $>10$ -s exposure) will experience a maximum although transient temperature increase in the retina of less than  $2^\circ\text{C}$  during a 50-s fixation trial. The large increase in the International Commission on Non-Ionizing Radiation Protection (ICNIRP) and ANSI Z136.1 safety limits for a long-duration small-source exposure to visible continuous wave lasers that was adopted in 2000 therefore appears appropriate. © 2004 Society of Photo-Optical Instrumentation Engineers. [DOI: 10.1117/1.1783355]

Keywords: laser; retina; eye movement; maximum permissible exposure; thermal damage; computer model.

Paper JBO-03122 received Oct. 14, 2003; revised manuscript received Feb. 19, 2004; accepted for publication Feb. 20, 2004.

## 1 Introduction

In 2000, the maximum permissible exposure (MPE) safe limit for long-duration exposure to laser radiation was amended.<sup>1,2</sup> This change resulted in a significant increase in the small-source MPE over that defined by the previous<sup>3</sup> safety standard of 1993. Figure 1 compares the current and previous MPE values for an 8-h exposure in the visible wavelength region ( $\lambda = 400$  to  $700$  nm). The increase in the MPE values is two to three orders of magnitude over most of the visible wavelengths.

One of the factors contributing to the decision to raise the MPE limits was a study of eye movements during fixation performed by Ness et al.<sup>4</sup> Eye (and head) movements affect the distribution of energy deposited in the retina. It was found that, for a 100-s fixation trial, the peak radiant exposure at the retina might be reduced to  $\sim 1/5$  the peak radiant exposure that would be experienced in a completely stationary eye.

Ness et al.,<sup>4</sup> recorded the small-scale eye movements of volunteers fixating on effectively a point source produced by a light-emitting diode (LED). The diode was very dim—each volunteer's eye was subject to a corneal irradiance of  $\sim 1 \text{ pW cm}^{-2}$ . Lund et al.<sup>5</sup> extended the study to higher in-

tensity sources by replacing the diode with a helium-neon (HeNe) laser ( $\lambda = 632.8$  nm). Attenuators were used so that the fixation source produced corneal irradiance values in the range  $0.6 \text{ pW cm}^{-2}$  to  $6 \text{ }\mu\text{W cm}^{-2}$ . No significant change in the tightness of the fixation pattern was observed as the source intensity increased.

From the eye movement data and reasonable assumptions about the laser beam's irradiance profile, the distribution of the radiant exposure at the retina can be determined.<sup>4</sup> This knowledge is adequate to predict the retinal damage threat from long-duration exposure to shorter wavelengths ( $\lambda < 540$  nm), where the damage process is usually photochemical in nature.<sup>6</sup> For photochemical damage, a constant dose (retinal radiant exposure) is required to elicit a damage response. However, for longer wavelengths ( $540 \text{ nm} < \lambda < 1400$  nm), the damage mechanism is predominantly the thermal denaturation of proteins.<sup>6</sup> The rate of this denaturation reaction is strongly temperature dependent,<sup>7</sup> and therefore detailed information about the thermal history of the retina is required to predict the onset of injury.

Although centrally peaked, the eye movement pattern during a 50-s fixation trial will typically move the retinal image of the laser source over a region that is greater than  $300 \text{ }\mu\text{m}$  in extent.<sup>5</sup> For retinal laser spot sizes on the order of 10s of

Address all correspondence to Brian J. Lund, c/o USAMRD-WRAIR, 7695 Dave Erwin Drive, Brooks City-Base, Texas 78235-5108, USA. Tel: 210-536-4648; Fax: 210-536-3450; E-mail: brian.lund@brooks.af.mil

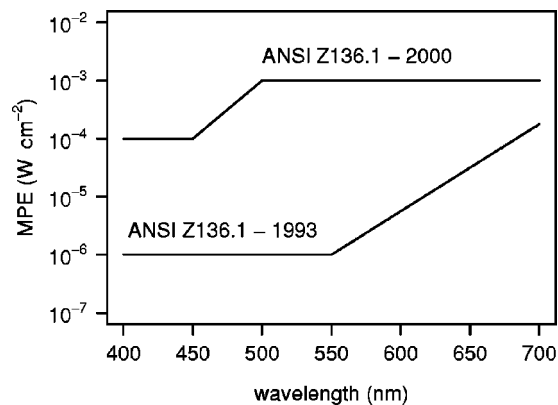


**Fig. 1** Change in the MPE for long-duration ( $>10^4$  s) viewing of a continuous wave laser source. The plot shows the MPE values for exposure to a small (minimum angular subtense) source (from Refs. 1, 2, and 3).

micrometers in diameter, the eye movements are large enough that a particular location on the retina will experience periods in which it is directly irradiated by the beam, and will therefore be heated. The same location will also experience periods when it is not directly illuminated by the beam, and will have an opportunity to cool.

Previous analytical and computational models of heating in the retina during a laser exposure (e.g., Refs. 8, 9, 10, and 11) have treated the retina as stationary, and using cylindrical symmetry, have reduced the problem to two spatial dimensions. This treatment is reasonable for short-duration exposures, i.e., single pulses, but not for the long-duration exposures of concern here. For the long-duration exposures, a detailed study of the effect of the eye movements on the thermal history of the retina is necessary.

A computer program called RHME (Retinal Heating in Moving Eye) was developed to simulate the heating in the retina during a long-duration fixation on a laser source. The primary goal of RHME is to compare the retinal thermal history in a moving eye to the heating pattern that would be experienced by a stationary eye. The program is also required to have a reasonable execution time ( $\sim$  few hours) on a desktop computer. Thus, simplifying assumptions were made about the geometry as well as the thermal and light-absorbing properties near the retina. The light source is also treated in a simple manner. Emphasis was placed on handling a source that is being moved about the retina due to eye movements.

Simulation results are presented for a small-source MPE-level exposure. Extended-source exposures will be examined in future work.

## 2 Model

The geometry of the RHME simulation is illustrated in Fig. 2. In this model, the eye is crudely separated into three regions. The retinal pigment epithelium (RPE) is modeled as a flat slab  $10\ \mu\text{m}$  thick centered on the  $z=0$  plane. The semi-infinite volume above the RPE represents the interior media of the eye through which light passes on the way from the cornea to the retina. The semi-infinite volume below the RPE represents post-RPE tissue, such as the choroid, sclera, etc.

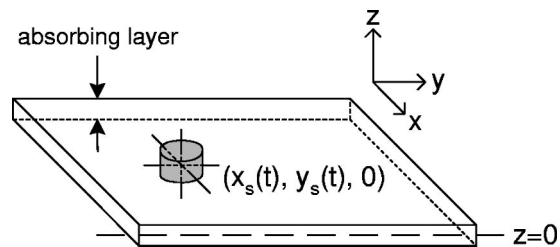


**Fig. 2** Geometry of the RHME model; the  $z=0$  plane bisects the RPE slab.

Light-absorbing melanin is<sup>12</sup> concentrated in the RPE. To simplify the calculations, light absorption is assumed to take place only in the RPE layer; heating due to light absorption in the pre- and post-RPE tissue is considered negligible in this model. Contributions to heating due to light scattered from the main light beam (large-angle scattering) are ignored. Although the primary location for light absorption is the melanin granules, the long exposure duration and low power of concern here mean that the RPE can be treated as a homogeneous material.

The ocular media in the model are assumed to have the density, specific heat, and thermal conductivity of water (see Table 1). These properties are taken to be homogeneous and isotropic. Light transmission and absorption characteristics are wavelength dependent and are extracted from the literature.<sup>12,13</sup>

A circular laser beam having a uniform irradiance profile (“top hat” beam profile) is incident on the RPE. The center of this beam spot traces out a path  $[x(t), y(t)]$  in accordance with eye movement data recorded during fixation.<sup>5</sup> Light is absorbed within a cylindrical volume as the beam passes through the RPE layer. The height of this absorbing volume is equal to the thickness of the RPE layer, while the diameter is equal to the diameter of the incident beam. The thickness of

**Table 1** Parameters used in the simulation.

Properties of Medium	
Thermal conductivity	$k=0.0063\ \text{J cm}^{-1}\ \text{s}^{-1}\ ^\circ\text{C}^{-1}$
Specific heat	$C=4.184\ \text{J g}^{-1}\ ^\circ\text{C}^{-1}$
Density	$\rho=1.0\ \text{g cm}^{-3}$
Thermal diffusivity	$\alpha=k/C\rho=0.0015\ \text{cm}^2\ \text{s}^{-1}$
RPE thickness	$h=10\ \mu\text{m}$
Beam Properties	
Irradiance at cornea <sup>a</sup>	$1.0\ \text{mW cm}^{-2}$
Ocular transmittance at $\lambda=632.8\ \text{nm}$	0.65
Absorption in RPE at $\lambda=632.8\ \text{nm}$	0.29
Power absorbed in RPE	$72.5\ \mu\text{W}$
Beam radius at RPE	$a=12.5\ \mu\text{m}$ ( $d=25\ \mu\text{m}$ )

<sup>a</sup> Averaged over a 7-mm-diam pupil.

the RPE is taken to be 10  $\mu\text{m}$ , as has been customary in previous models.<sup>6–11</sup> Energy absorbed is converted to heat and used as the source term in the heat conduction equation (see later). Note that the energy deposition is assumed to be uniform throughout the thickness of the RPE layer—there is no Beer's law attenuation calculation.

The uniform energy deposition, coupled with the simplified geometry of the simulation, means there is a symmetry about the  $z=0$  plane in this model. This symmetry is exploited in the computer program to reduce the memory and computational requirements.

Temperature increase throughout the model space is calculated by solving the standard heat conduction equation for an isotropic, homogeneous medium:<sup>14</sup>

$$\rho C \frac{\partial \theta}{\partial t} - k \nabla^2 \theta(x, y, z, t) = Q(x, y, z, t). \quad (1)$$

Here  $\theta$  is the temperature increase in degrees centigrade,  $\rho$  is the density in  $\text{g cm}^{-3}$ ,  $C$  is the specific heat in  $\text{J g}^{-1} \text{ } ^\circ\text{C}^{-1}$ , and  $k$  is the thermal conductivity in  $\text{J cm}^{-1} \text{ s}^{-1} \text{ } ^\circ\text{C}^{-1}$ . The heat source term  $Q$  ( $\text{J cm}^{-3} \text{ s}^{-1}$ ) represents the cylindrical absorbing volume in the RPE—its magnitude is constant, but its position traces out a path determined by eye movements. RHME imposes the boundary condition  $\theta(|\mathbf{r}|, t) = 0$  as  $|\mathbf{r}| \rightarrow \infty$ .

The heat conduction equation is solved numerically using the 3-D finite element method.<sup>15–17</sup> The temperature rise distribution is expanded using linear interpolating functions over a 3-D spatial mesh. The finite elements defined on this mesh are regular rectangular solids. An implicit time-stepping procedure is used to calculate the time evolution of the temperature rise distribution from the initial conditions  $\theta(x, y, z, t = 0) = 0$ . The inputs to the program include the density, specific heat, and thermal conductivity of the model eye medium; the diameter of the beam spot at the RPE; the total power deposited into the RPE (given in watts); and the path of the source about the plane of the RPE  $[x(t), y(t)]$ . The latter is extracted from experimentally recorded fixation data.<sup>5</sup> The output of the program is the temperature rise  $\theta(x, y, z)$  at specified time intervals; the maximum temperature rise  $\theta_{\max}(x, y, z)$  observed throughout the trial simulation

$$\theta_{\max}(x, y, z) = \max\{\theta(x, y, z, t); 0 \leq t \leq t_{\text{trial}}\}, \quad (2)$$

and the time-averaged temperature rise,

$$\theta_{\text{avg}}(x, y, z) = \frac{1}{t_{\text{trial}}} \int_0^{t_{\text{trial}}} \theta(x, y, z, t') dt'. \quad (3)$$

## 2.1 Parameters

The parameters used for the simulation results presented in this paper are listed in Table 1.

In current safety standards,<sup>1,2</sup> the MPE for a long-duration small-source ocular exposure to a continuous wave laser is  $1 \text{ mW cm}^{-2}$  for visible wavelengths. The MPE value is defined as the corneal irradiance averaged over a 7-mm-diam pupil. An MPE-level exposure therefore admits a total interocular power (TIP) of  $(1 \text{ mW cm}^{-2}) [\pi(0.7 \text{ cm}/2)^2] = 385 \mu\text{W}$ .

At the wavelength  $\lambda = 632.8 \text{ nm}$  (such as from the HeNe laser used by Lund et al.<sup>5</sup>), the direct transmittance through the ocular medium to the RPE is<sup>13</sup>  $\sim 65\%$ . Absorption in the RPE at this wavelength is<sup>12</sup>  $\sim 29\%$ . Therefore, the power absorbed in the RPE during exposure to a  $1 \text{ mW cm}^{-2}$  corneal irradiance beam at  $\lambda = 632.8 \text{ nm}$  is approximately  $P_{\text{RPE}} = (385 \mu\text{W})(0.65)(0.29) = 72.5 \mu\text{W}$ . For the simulation results presented here, a value of  $P_{\text{RPE}} = 72.5 \mu\text{W}$  is used.

A beam spot diameter of  $25 \mu\text{m}$  is used for all results presented here. This retinal spot diameter corresponds to a visual angle of  $1.5 \text{ mrad}$ , which is equal to  $\alpha_{\min}$ , the limiting angular subtense separating a small source from extended source viewing in the safety standards.<sup>1,2</sup>

## 3 Results

### 3.1 Stationary Source

For a stationary cylindrical heat source, an analytical solution of Eq. (1) can be obtained.<sup>18</sup> This solution is in terms of a double integral over the radial distance from the cylinder axis, and the exposure duration. In the  $z=0$  plane, the solution reduces to

$$\theta(r, z=0, t) = \frac{Q_0}{2\alpha} \int_0^t \frac{\exp(-r^2/4\alpha t')}{t'} \int_0^a \exp\left(\frac{-r'^2}{4\alpha t'}\right) \times I_0\left(\frac{rr'}{2\alpha t'}\right) \text{erf}\left(\frac{l}{2\sqrt{\alpha t'}}\right) r' dr' dt', \quad (4)$$

where  $r = (x^2 + y^2)^{1/2}$  is the radial distance from the cylinder axis ( $z$  axis),  $a$  is the cylinder radius,  $2l$  is the cylinder height,  $\alpha = k/\rho C$  is the thermal diffusivity,  $Q_0$  is the strength of the heat source, and  $I_0$  is a modified Bessel function. At  $r=0$ , the preceding equation reduces to

$$\theta(r=0, z=0, t) = Q_0 \int_0^t \left[1 - \exp\left(\frac{-a^2}{4\alpha t'}\right)\right] \text{erf}\left(\frac{l}{2\sqrt{\alpha t'}}\right) dt'. \quad (5)$$

Equations (4) and (5) can be integrated numerically to provide checks on the performance of the simulation.

The results of running RHME for a small-diameter stationary source [no eye movements,  $x(t) = y(t) = 0$ ] for a 50-s exposure are shown in Figs. 3 and 4. Note that the peak temperature rise in the plane at  $z=0$ , 5, and  $10 \mu\text{m}$  was 1.14, 0.93, and  $0.61^\circ\text{C}$ , respectively. Figure 3(a) shows the maximum temperature rise  $\theta(x, y, z=0, t=50 \text{ s})$  in the plane  $z=0$ . Due to the symmetry of the simulation geometry, the plane  $z=0$  is where the greatest temperature increase will occur. As expected from the cylindrical symmetry of this particular situation, the temperature contours are circular and symmetric about the location of the source ( $x=0, y=0$ ).

The temperature rise in the  $z=5 \mu\text{m}$  plane is shown in Fig. 3(b). This is the extent in the  $z$  direction of the cylindrical absorption region of the RPE model (thickness =  $10 \mu\text{m}$ ). Figure 3(c) is the temperature rise in the  $z=10 \mu\text{m}$  plane, which is outside the light-absorbing volume. It is therefore only indirectly heated through thermal diffusion from the absorbing cylindrical volume.

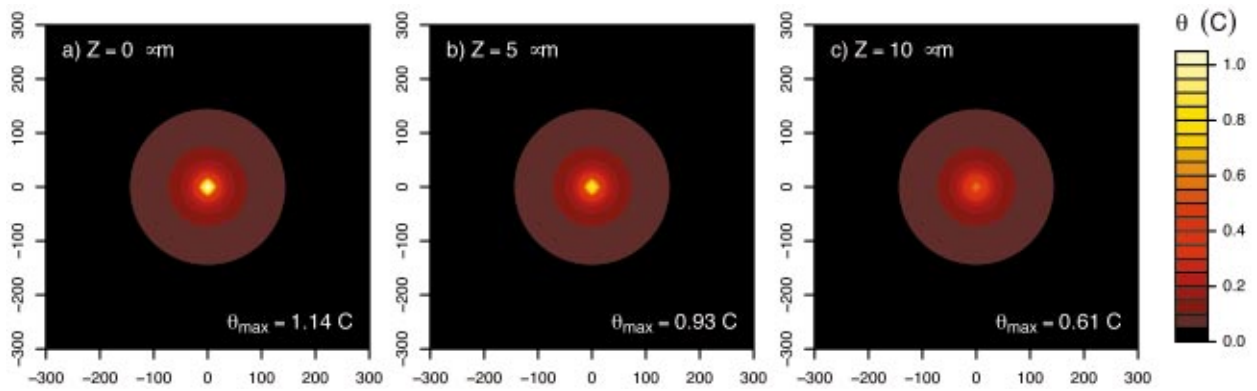


**Fig. 3** Temperature increase, in degrees centigrade, after a 50-s exposure for a stationary small source. Source characteristics are listed in Table 2 in Sec. 3.2. The horizontal axis in the figures represents the nasal/temporal (horizontal) position on the retina, in micrometers. The vertical axis represents the superior/inferior (vertical) position.

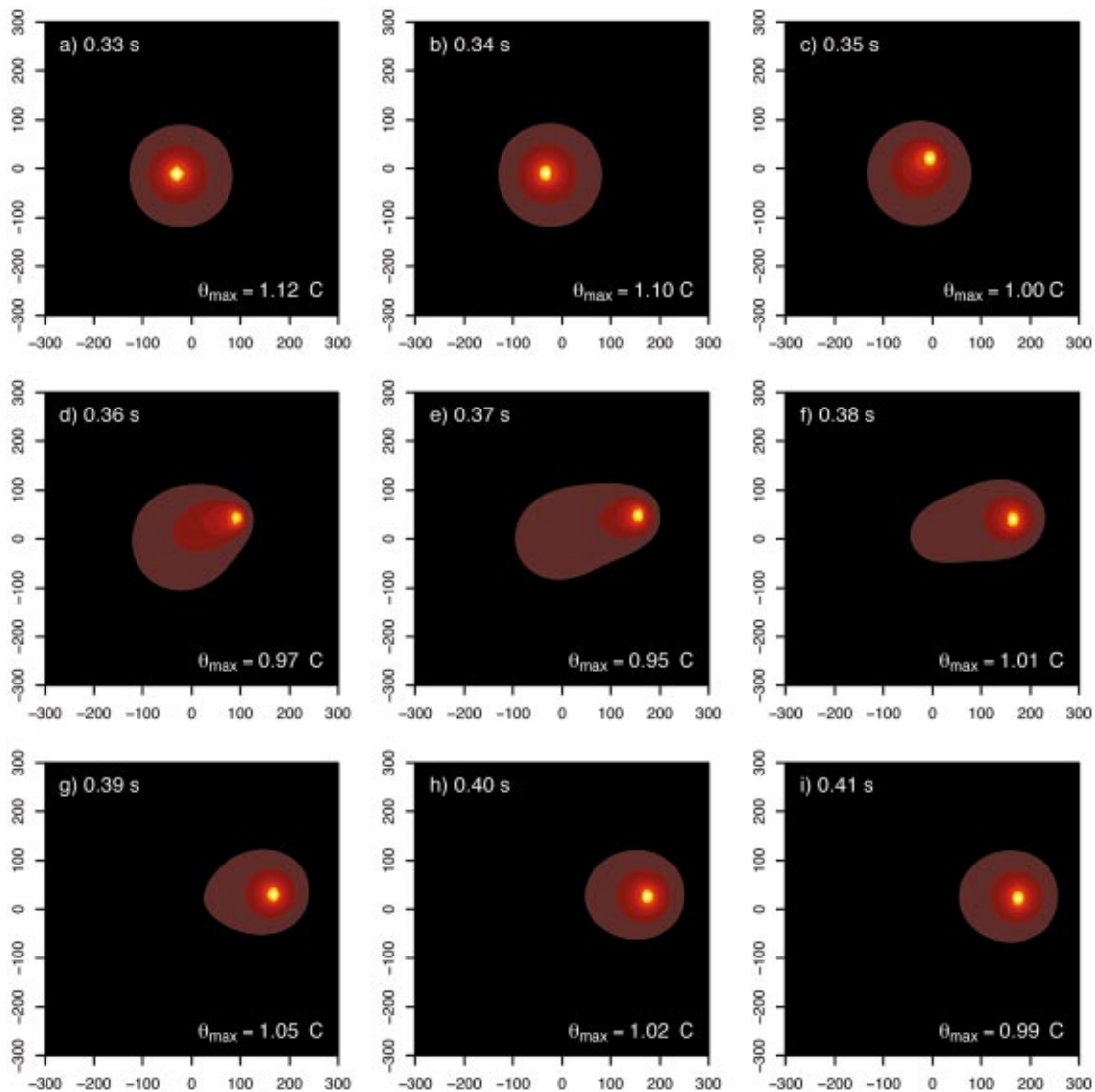


**Fig. 6** Response of the temperature in the retina ( $z=0$  plane) to source movement, with eye movement data from subject 6 of Lund et al.<sup>5</sup> [Fig. 5(c)], during a microsaccade (flick).

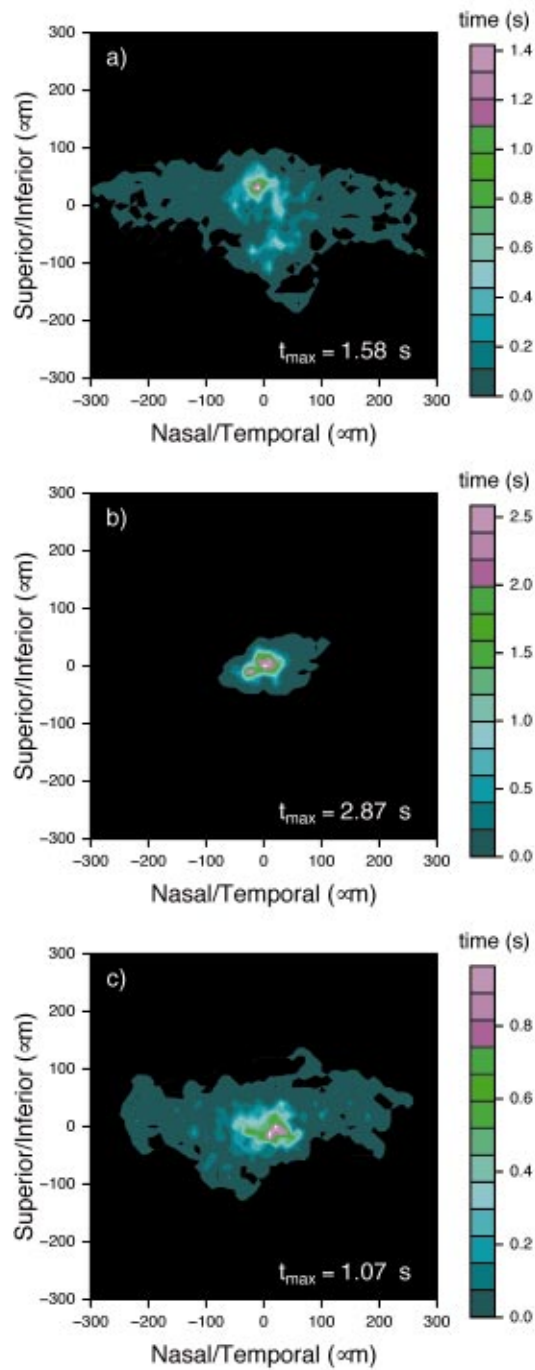


**Fig. 5** Eye movement visitation plots illustrating the extent of eye movements during the fixation task. Minimum contour in these plots = 0.001 s. Note the time scales are different for each figure. 300  $\mu\text{m}$  on the retina corresponds to  $\sim 1$  deg in the field of view. (a) Subject 1, fixate for 50 s on HeNe source producing a corneal irradiance of  $0.6 \text{ pW cm}^{-2}$ ; (b) subject 4, 50 s,  $60 \text{ pW cm}^{-2}$ ; and (c) subject 6, 45 s,  $6 \text{ } \mu\text{W cm}^{-2}$ . (Data from Lund et al.<sup>5</sup>)



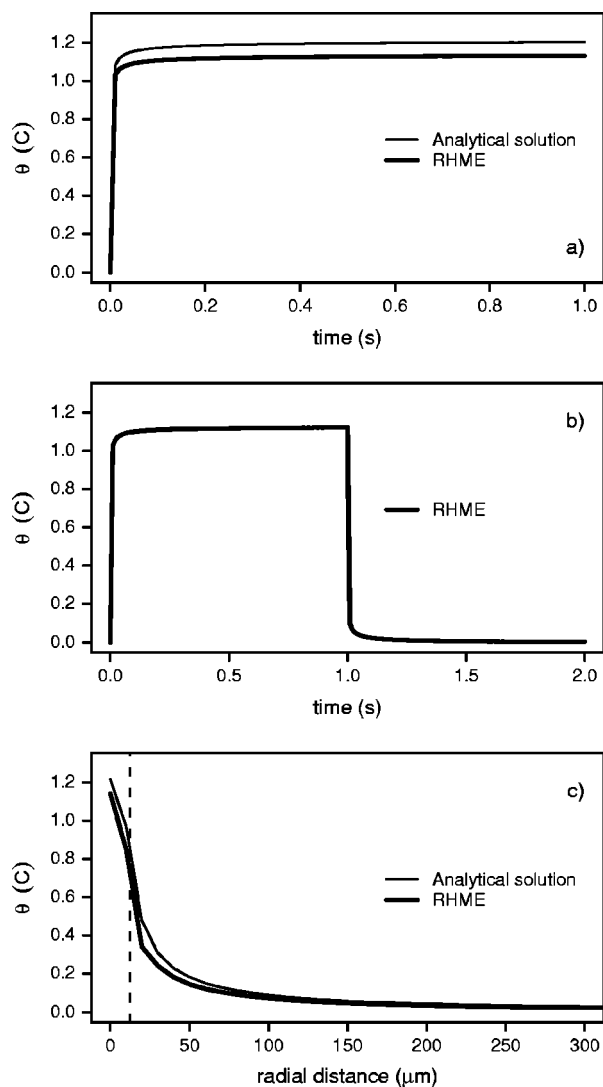


**Fig. 4** Comparison of the RHME simulation and the analytical solution for a stationary small source centered at the retinal position ( $x = 0 \mu\text{m}$ ,  $y = 0 \mu\text{m}$ ,  $z = 0 \mu\text{m}$ ). (a) temperature rise versus time at the retinal location ( $x = 0$ ,  $y = 0$ ,  $z = 0$ ). RHME underpredicts the analytical solution by about 6%. At 10 ms,  $\theta_{\text{RHME}} = 1.03^\circ\text{C}$ , 90% of its value at 0.5 s [ $\theta_{\text{RHME}}(0.5 \text{ s}) = 1.13^\circ\text{C}$ ]. (b) RHME simulation for a stationary source that is turned on at  $t = 0$  s and turned off at  $t = 1.0$  s. (c) Temperature rise versus radial distance in the  $z = 0$  plane at  $t = 50$  s. The dashed line indicates the edge of the source volume.

Figure 4(a) shows the temperature rise during the first 1 s of exposure at the center of the cylindrical absorbing volume, ( $x = 0$ ,  $y = 0$ ,  $z = 0$ ). The results of the RHME simulation are compared to the analytical solution at this point [Eq. (5)]. The computer simulation underpredicts the analytical solution by  $\sim 6\%$ .

The rapid temperature increase observed in Fig. 4 is important. Within about 10 ms, the temperature at this central point has risen to within 90% of the final temperature it will attain after a 50-s exposure [ $\theta_{\text{RHME}}(0.01 \text{ s}) = 1.03^\circ\text{C}$ ,  $\theta_{\text{RHME}}(50 \text{ s}) = 1.14^\circ\text{C}$ ]. This means that once a particular location on the retina becomes directly exposed to the beam, it will rapidly heat to a temperature near the maximum it would reach if continuously and constantly exposed. Cooling once

**Table 2** Comparison of simulation results for small-source exposure.

	Fixation Ellipse Area ( $\mu\text{m}^2$ )	Peak $\theta_{\text{max}}$ ( $^\circ\text{C}$ )	Peak $\theta_{\text{avg}}$ ( $^\circ\text{C}$ )
Stationary	0.0	1.14	1.14
Subject 1	6552	1.23	0.24
Subject 4	951	1.21	0.42
Subject 6	4033	1.15	0.25

the source is removed from a location (or the laser beam moves away due to eye movements) is also rapid, as can be seen in Fig. 4(b). This figure is again a plot of the temperature rise at the point ( $x = 0$ ,  $y = 0$ ,  $z = 0$ ). The heat source (i.e., the laser) is turned on at time  $t = 0$  s, and turned off at  $t = 1.0$  s.

Figure 4(c) shows the radial distribution of the temperature rise in the  $z = 0$  plane after a 50-s exposure to a stationary source. The RHME model is seen to underpredict the analytical solution for a stationary source [Eq. (4)]. It was expected that there would be a limit on the accuracy of the simulation—the use of linear interpolation functions on any practical (i.e., reasonable run time) mesh cannot accurately represent the temperature distribution in the regions near the boundary of the heat source (absorbing volume in the RPE). The heat source, by its definition in this model, has an infinite slope at its boundary. However, the accuracy attained is deemed sufficient for the goals of the simulation—to investigate how eye movements affect the thermal history of the retina during a long-duration exposure to continuous laser light.

### 3.2 Eye Movement Data

Source movement data input into the simulation are taken from the fixation study of Lund et al.<sup>5</sup> Volunteers deliberately fixated on a spot produced by a HeNe laser ( $\lambda = 632.8 \text{ nm}$ ) for 50 s. This fixation target produced corneal irradiance values in the range  $0.6 \text{ pW cm}^{-2}$  to  $6 \mu\text{W cm}^{-2}$ . The head was stabilized using a forehead/chin rest combination. The data recording rate was 1000 Hz. The eye movement data were expressed in terms of retinal coordinates and were interpreted in terms of the path that the laser spot would follow as it was moved about the retina by eye movements. As such, these data could be directly inserted into the thermal model.

Figure 5 shows the eye movement patterns for which retinal heating simulation results are presented below. These “visitation plots” show the accumulated time, during a 50-s fixation trial, that eye movements would have placed the center of the laser beam at each point of the retina. The movement patterns are characterized by a “fixation ellipse” that is derived from the standard deviations of the nasal-temporal and superior-inferior eye movement data.<sup>5</sup> The area of the fixation ellipse gives a measure of the tightness of fixation during a given trial. Fixation ellipse areas are listed in Table 2. The eye movement patterns used here are examples of the loosest [subject 1, Fig. 5(a)] and tightest [subject 4, Fig. 5(b)] eye movement patterns observed.<sup>5</sup> The eye movement pattern

of subject 6 [Fig. 5(c)] exhibited unusually frequent and pronounced nasal-temporal microsaccades (flicks) during the trial shown here.

### 3.3 Simulations with Moving Eye

Figure 6 is a time sequence showing the simulation of the thermal response of the retina using the eye movement data of subject 6. These nine frames capture the temperature rise in the  $z=0$  plane during a microsaccade (flick) which moved the laser spot a distance of  $\sim 230 \mu\text{m}$  on the retina in 40 to 50  $\mu\text{s}$ . Because of the rapid thermal response times (of the order of 10  $\mu\text{s}$ , Fig. 4), only the region of the retina directly irradiated by the laser beam attains a significant temperature rise. Once the beam moves away from a particular point of the retina, it rapidly cools. In Fig. 6, it is easy to identify the location of the beam in each of the frames.

During relatively quiescent times in the eye movement pattern, such as just before [Fig. 6(a)] and just after [Fig. 6(i)] the microsaccade, the temperature rise distribution is nearly circular, similar to that obtained for a stationary source (Fig. 3). Only during periods of rapid and large-scale eye movement does the temperature rise pattern show an asymmetry [Figs. 6(c) to 6(g)].

Because of the rapid thermal response, all points of the retina directly exposed to the beam (due to the eye movements) will, at some time during the fixation period, be heated to a temperature near that of the maximum temperature reached for the stationary source. Thus, it is expected that a plot of the maximum temperature rise distribution [Eq. (2)] for, say, the  $z=0$  plane, will be a plateau or mesa having roughly the same shape as the overall eye movement pattern (Fig. 5). This is indeed the case, as illustrated in Figs. 7, 8, and 9. In Figs. 7(a), 8(a), and 9(a) the contour lines of the visitation time (eye movement) distributions of Fig. 5 are superimposed on the maximum temperature rise distributions for each of the three subjects considered.

Another consequence of the rapid thermal response time is that the time-averaged temperature rise distribution, defined by Eq. (3), should reflect the eye movements. Once again, this is clearly seen to be the case in Figs. 7, 8, and 9, where the peaks of the average temperature rise distribution mimic the peaks in the visitation time plots. Note that subject 4 (Fig. 8), whose eye movement pattern is the tightest, reaches a higher peak average temperature rise than do the other two subjects.

Table 2 lists the peak value in the  $\theta_{\text{max}}$  and  $\theta_{\text{avg}}$  distributions in the  $z=0$  plane for the stationary source and the three sets of eye movement data. Also listed is the area of the fixation ellipse for each data set. The peak of the  $\theta_{\text{avg}}$  distribution is seen to have a strong and inverse relation with the fixation ellipse area. The peak of the  $\theta_{\text{max}}$  distribution is relatively insensitive to the nature of the eye movements. (The variation here may be another indication of the accuracy of the simulation.)

The smoothness of the average temperature rise plots hides the complex thermal history of a given point of the retina. The temperature rise at the location of the peak value of  $\theta_{\text{avg}}$  is plotted as a function of time in Fig. 10 for the three eye movement data sets. These traces clearly exhibit the periods of higher temperature when the particular retinal location is directly exposed (or nearly so) to the laser. The lower tem-

perature regions occur when, due to the eye movements, the laser spot is moved some distance away.

## 4 Discussion

It is the complicated thermal history, as illustrated in Fig. 10, that must be analyzed when trying to understand whether an individual is at risk of receiving a thermal injury to the retina during a long-duration exposure to a laser. Thermal damage is understood to be the result of protein denaturation and enzyme deactivation.<sup>6</sup> This damage process is usually modeled as a first-order rate process, which can be quantified by calculating the parameter  $\Omega$  from an Arrhenius integral:<sup>7</sup>

$$\Omega(\mathbf{r}, t) = A \int_0^t \exp[-E_a/RT(\mathbf{r}, t')] dt'. \quad (6)$$

In Eq. (6),  $A$  is a frequency factor in inverse seconds,  $t$  is the total exposure time,  $E_a$  is the energy of activation ( $\text{J mole}^{-1}$ ),  $R$  is the universal gas constant ( $8.32 \text{ J mole}^{-1} \text{ K}^{-1}$ ), and  $T(\mathbf{r}, t)$  is the (time-dependent) absolute temperature in Kelvins at the point  $\mathbf{r}$ . The parameters  $A$ ,  $E_a$ , and  $R$  are often determined by fits to damage threshold data so that the value  $\Omega = 1$  indicates irreversible damage. The presence of the temperature in the exponent of the integrand indicates that the thermal damage process is very sensitive to temperature. A particular retinal location attains the same maximum temperature in the stationary and moving eyes. However, because eye movements will remove the retinal location from direct exposure to the beam, cooling of the particular spot will occur. Therefore, it can be expected that a significantly longer duration exposure is needed in the moving eye before accumulated thermal damage becomes permanent and irreversible.

The temperature increases calculated for an MPE-level exposure to light from a HeNe laser ( $\lambda = 632.8 \text{ nm}$ ) are fairly small,  $\theta_{\text{max}} \sim 1.2^\circ\text{C}$ . This result is desirable for exposure levels that are deemed safe. The current version of RHME does not incorporate a damage assessment model, such as Eq. (6). A detailed investigation of thermal damage thresholds requires either the addition of such a model to RHME, or the development of a model that can make use of the output of RHME (say, e.g., the temperature-time curves of Fig. 10). Work in this direction is currently in progress.

The simulation results presented here were calculated for an MPE-level exposure to a continuous wave HeNe laser. The program itself does no beam transport calculations and is ignorant of any wavelength dependencies. To determine the power deposited in the model RPE (in this case,  $72.5 \mu\text{W}$ ), ocular transmission and RPE absorption coefficients for  $\lambda = 632.8 \text{ nm}$  were used. Figure 11 is a plot of the direct ocular transmission coefficient<sup>13</sup>  $T_{\text{ocular}}$  and the RPE absorption coefficient<sup>12</sup>  $A_{\text{RPE}}$  for the visible wavelength region. The product  $A_{\text{RPE}} \times T_{\text{ocular}}$  gives the fraction of the TIP that is absorbed by the RPE, and therefore the strength of the source term used in the RHME model. For wavelengths greater than 500 nm (where the MPE is  $1 \text{ mW cm}^{-2}$ , see Fig. 1),  $A_{\text{RPE}} \times T_{\text{ocular}}$  is nearly linearly decreasing from a value of 0.29 at  $\lambda = 550 \text{ nm}$  down to a value of 0.15 at  $\lambda = 700 \text{ nm}$ . (Note that  $A_{\text{RPE}} \times T_{\text{ocular}} = 0.19$  at  $\lambda = 632.8 \text{ nm}$ .) Because the thermal diffusion equation is linear in the source term  $Q$  as well as the temperature increase  $\theta$ , an estimate of the temperature in-

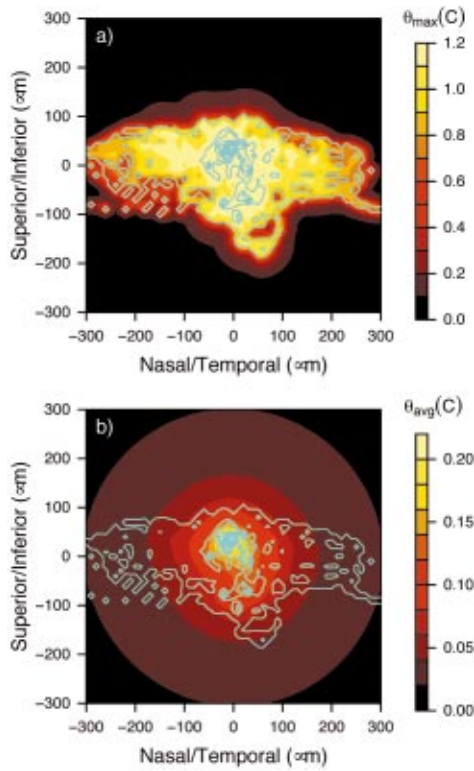


**Fig. 7** Eye movement pattern [visitation time contour plot, Fig. 5(a)] superimposed over (a) maximum temperature increase and (b) time-averaged temperature increase in the  $z=0$  plane, for subject 1 of Lund et al.<sup>5</sup> Calculations are for a MPE-level exposure (see Table 1).

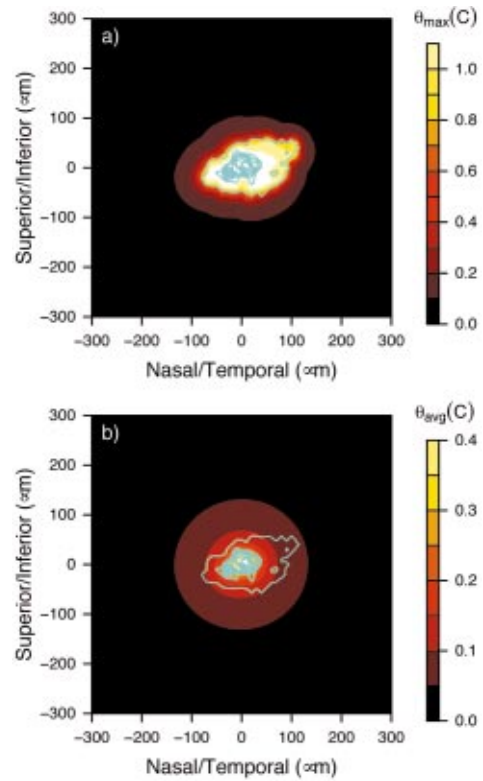


**Fig. 8** Eye movement pattern [Fig. 5(b)] superimposed over (a) maximum temperature increase and (b) time-averaged temperature increase in the  $z=0$  plane, for subject 4.

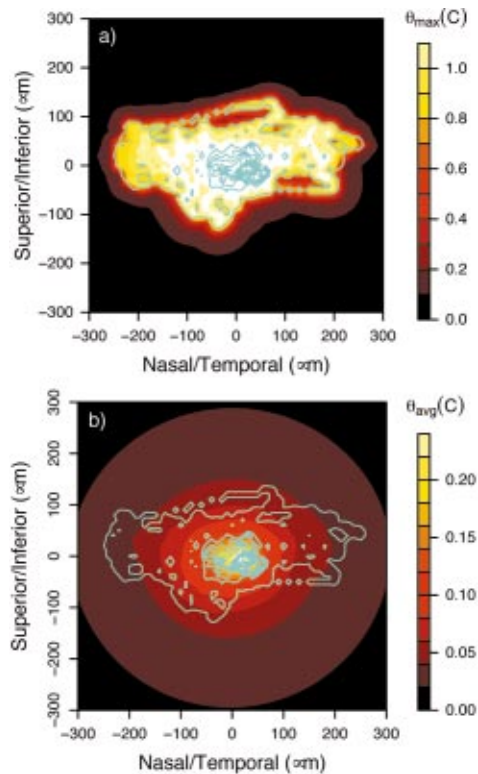


**Fig. 9** Eye movement pattern [Fig. 5(c)] superimposed over (a) maximum temperature increase and (b) time-averaged temperature increase in the  $z=0$  plane, for subject 6.



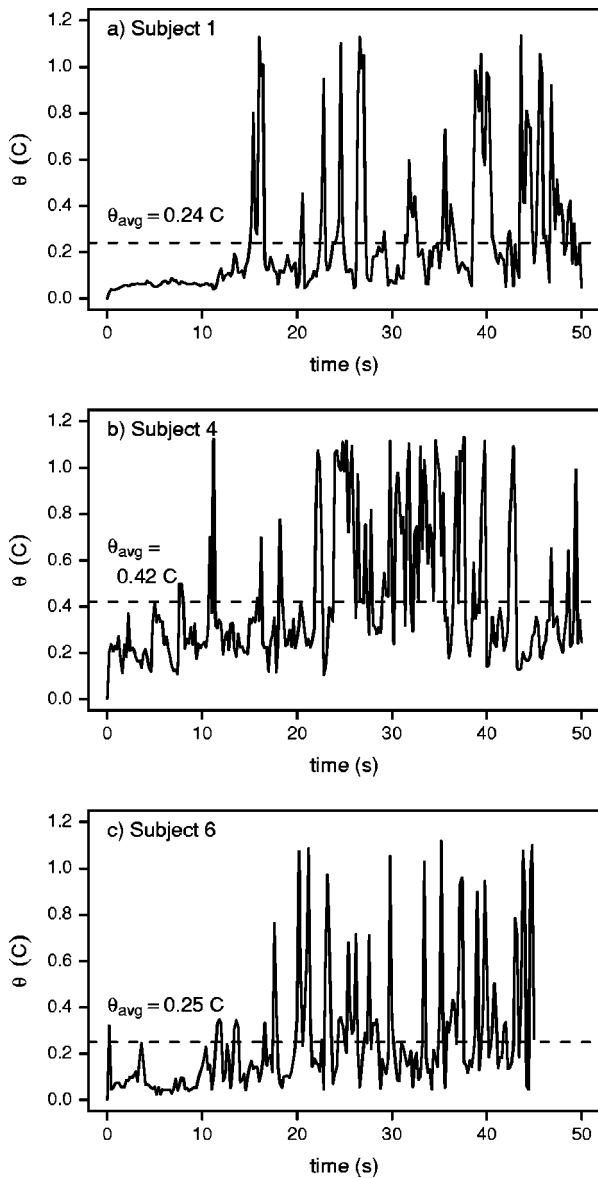


**Fig. 10** Temperature increase versus time at the location of the peak of the time-averaged temperature rise distributions in the  $z=0$  plane for (a) subject 1, 50 s,  $\theta_{\max}=1.14^{\circ}\text{C}$ ,  $\theta_{\text{avg}}=0.24^{\circ}\text{C}$ ; (b) subject 4, 50 s,  $\theta_{\max}=1.13^{\circ}\text{C}$ ,  $\theta_{\text{avg}}=0.42^{\circ}\text{C}$ ; and (c) subject 6, 45 s,  $\theta_{\max}=1.13^{\circ}\text{C}$ ,  $\theta_{\text{avg}}=0.25^{\circ}\text{C}$ .

crease that would occur during  $1\text{ mW cm}^{-2}$  corneal irradiance exposures to other wavelengths can be obtained by scaling the results from the  $\lambda=632.8\text{ nm}$  calculations. The slow variation of  $A_{\text{RPE}} \times T_{\text{ocular}}$  with wavelength indicates that the maximum temperature increase will be of the same order of magnitude as that calculated at  $\lambda=632.8\text{ nm}$ . Specifically,  $\theta_{\max}(\lambda=500\text{ nm}) \approx (0.29/0.19) \cdot 1.2^{\circ}\text{C} = 1.8^{\circ}\text{C}$  for an exposure which produces a corneal irradiance of  $1\text{ mW cm}^{-2}$ . Similarly,  $\theta_{\max}(\lambda=700\text{ nm}) \approx 0.95^{\circ}\text{C}$ .

The RHME program was written to examine the effect eye movements have on the retinal heating pattern during a long-duration exposure. The model has been kept simple to reduce computational effort, and thus the time required for the program to run. All absorption leading to a significant tempera-

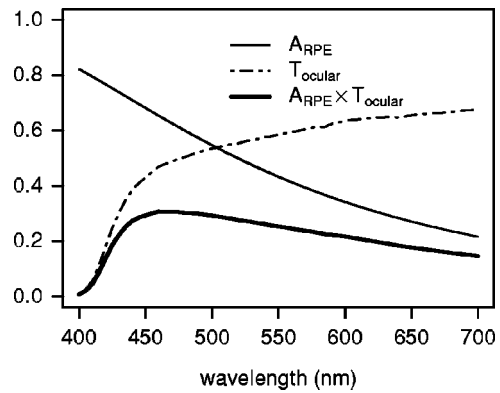


**Fig. 11** RPE absorption coefficient  $A_{\text{RPE}}$  and direct ocular transmission coefficient  $T_{\text{ocular}}$  as a function of wavelength for visible light. The product of these two coefficients gives the percentage of the TIP that is absorbed in the RPE ( $A_{\text{RPE}}$  absorption from Gabel et al.,<sup>12</sup>  $T_{\text{ocular}}$  from Boettner and Wolter<sup>13</sup>).

ture increase is assumed to take place within the RPE. Energy absorption within the choroid, which does contain some melanin, was neglected. While the absorption at a given wavelength by the RPE and the choroid are comparable,<sup>19</sup> the choroid is of the order of 10 times thicker than the RPE. The density of energy deposited per unit time ( $\text{J cm}^{-3}\text{ s}^{-1}$ ) is thus an order of magnitude smaller in the choroid than in the RPE (see also Ref. 10). Temperature increase in the retina is therefore dominated by energy absorption within and diffusion of heat from the RPE.

Welch et al.<sup>20</sup> and Birngruber<sup>9</sup> developed a simple model to investigate the significance of choroidal blood flow on temperature calculations for laser-irradiated tissue. Their results indicate that blood flow will have a negligible effect on the simulation results presented here (50-s exposure to a minimum spot size beam). For large spot sizes or much longer duration exposures, heat transport due to blood flow will lower the temperature below that predicted by the simple RHME model. In this sense, the RHME model can be considered conservative in that it overestimates the potential for thermal damage to occur.

The eye movement data used for the simulation results presented here represent a “worst-case” scenario from a laser perspective—subjects, with fixed head position, deliberately staring into a laser beam. Yet the RHME simulation results indicate that the maximum temperature increase is less than  $2^{\circ}\text{C}$  when experiencing an exposure to a (visible wavelength) small source producing a corneal irradiance of  $1\text{ mW cm}^{-2}$ . This is an extremely bright light source. For comparison, recall that the eye movement data for Subject 6 [Fig. 5(c)] was recorded while that individual stared at a source of  $6\text{ }\mu\text{W cm}^{-2}$  corneal irradiance. The experience was likened to staring at the high beams of an oncoming vehicle.<sup>5</sup>

The relatively low temperature increases calculated by the RHME simulation seem to indicate that the long-duration exposure limits for a continuous wave laser<sup>3</sup> were indeed overly conservative, and the greatly increased current small-source exposure limits<sup>1,2</sup> will be effective in preventing (thermal) injury, which requires<sup>6–11</sup> a temperature increase of at least 10 to  $20^{\circ}\text{C}$ .

## 5 Conclusion

The computer program RHME was developed to investigate the effect of eye movements on the thermal history of the retina during a long-duration exposure to a continuous laser source. For a small-source exposure, the results of the simulation indicate that the maximum temperature reached in the retina is independent of the eye movement pattern, but depends only on the source characteristics. The time-averaged temperature, however, is strongly determined by the eye movement pattern, as is the thermal history of a particular location in the retina.

The thermal history for a particular retinal location may be complex, as the location heats when directly exposed to the laser beam, and cools when eye movements shift the laser spot to a new retinal location. This complex thermal history must be examined to determine the likelihood of receiving thermal damage during a long-duration exposure to continuous wave laser light.

For an MPE to a HeNe laser ( $1 \text{ mW cm}^{-2}$  corneal irradiance,  $\lambda = 632.8 \text{ nm}$ ) producing a minimal retinal spot of  $25 \mu\text{m}$  in diameter, RHME estimates a maximum temperature increase of  $\sim 1.2^\circ\text{C}$  in areas of the retina directly irradiated by the laser beam. This maximum temperature increase is sustained for only brief periods of time, until eye movements move the image of the laser to a different location on the retina. The wavelength dependence of the ocular transmission and RPE absorption coefficients indicate that the maximum temperature increase will be less than  $2^\circ\text{C}$  for MPE-level exposures to visible wavelengths. This relatively small temperature increase calculated for such a bright source indicates that the increase in long-duration exposure limits for small sources that occurred<sup>1,2</sup> in 2000 was justified.

### Acknowledgments

This work was supported by U.S. Air Force Contract No. F46124-02-7003-0007, Task Order 07, entitled "Biomedical Assessment and Treatment for Laser Injury" awarded to Northrop Grumman Information Technology. Task Order 07 is sponsored by the U.S. Army Medical Research Detachment of the Walter Reed Army Institute of Research, Brooks City-Base, Texas. This work was conducted at the U.S. Army Medical Research Detachment, Brooks City-Base, Texas.

### Disclaimer

The opinions or assertions contained herein are the private views of the author and are not to be construed as official or as reflecting the views of Northrop Grumman IT, the Department of the Army, or the Department of Defense. Human Volunteers participated in the eye movement study after giving their free and informed voluntary consent. Investigators adhered to AR 70-25 and U.S. Army-Medical Research and Materiel Command (USAMRMC) Regulation 50-25 on the use of volunteers in research.

## References

1. American National Standards Institute (ANSI), *Safe Use of Lasers, Standard Z136.1*, Laser Institute of America, Orlando, FL (2000).
2. International Commission on Non-Ionizing Radiation Protection (IC-NIRP), "Revision of guidelines on limits of exposure to laser radiation of wavelengths between 400 nm and  $1.4 \mu\text{m}$ ," *Health Phys.* **79**(4), 431–440 (2000).
3. American National Standards Institute (ANSI), *Safe User of Lasers, Standard Z136.1*, Laser Institute of America, Orlando, FL (1993).
4. J. W. Ness, H. Zwick, B. E. Stuck, D. J. Lund, B. J. Lund, J. W. Molchany, and D. H. Sliney, "Retinal image motion during deliberate fixation: implications to laser safety for long duration viewing," *Health Phys.* **78**(2), 131–142 (2000).
5. B. J. Lund, H. Zwick, D. J. Lund, and B. E. Stuck, "Effect of source intensity on ability to fixate: implications for laser safety," *Health Phys.* **85**(5), 567–577 (2003).
6. D. Sliney and M. Wolbarsht, *Safety with Lasers and Other Optical Sources*, Plenum Press, New York and London (1980).
7. J. Pearce and S. Thomsen, "Rate process analysis of thermal damage," Chap. 17 in *Optical-Thermal Response of Laser-Irradiated Tissue*, A. J. Welch and M. J. C. van Gemert, Eds., pp. 561–606, Plenum Press, New York (1995).
8. R. Birngruber, F. Hillenkamp, and V.-P. Gabel, "Theoretical investigations of laser thermal retinal injury," *Health Phys.* **48**(6), 781–796 (1985).
9. R. Birngruber, "Choroidal circulation and heat convection at the fundus of the eye: implications for laser coagulation and the stabilization of retinal temperature," in *Laser Applications in Medicine and Biology*, Vol. 5, M. L. Wolbarsht, Ed., pp. 277–361, Plenum Press, New York, London (1991).
10. M. A. Mainster, T. J. White, J. H. Tips, and P. W. Wilson, "Retinal-temperature increases produced by intense light sources," *J. Opt. Soc. Am.* **60**(2), 264–270 (1970).
11. A. N. Takata, L. Goldfinch, J. K. Hinds, L. P. Kuan, N. Thomopoulos, and A. Weigandt, *Thermal Model of Laser-Induced Eye Damage*, Final Tech. Rep., Illinois Institute of Technology Research Institute (IITRI), J-TR 74-6324 (1974).
12. V.-P. Gabel, R. Birngruber, and F. Hillenkamp, "Visible and near infrared light absorption in pigment epithelium and choroid," in *Int. Congress Series*, No. 450: XXIII. Concilium. Ophthalmologicum, Kyoto, pp. 658–662, Oxford: Excerpta Medica, Amsterdam (1978).
13. E. A. Boettner and J. R. Wolter, "Transmission of the ocular media," *Invest. Ophthalmol.* **1**, 776–783 (1962).
14. H. S. Carslaw and J. C. Jaeger, *Conduction of Heat in Solids*, 2nd ed., Clarendon Press, Oxford (1959).
15. T. J. R. Hughes, *The Finite Element Method: Linear Static and Dynamic Finite Element Analysis*, Dover, Mineola, NY (2000).
16. K. H. Huebner, D. L. Dewhirst, D. E. Smith, and T. G. Byrom, *The Finite Element Method for Engineers*, 4th ed., Wiley, New York (2001).
17. J. N. Reddy and D. K. Gartling, *The Finite Element Method in Heat Transfer and Fluid Dynamics*, 2nd ed., CRC Press, Boca Raton, FL (2001).
18. J. Roider and R. Birngruber, "Solution of the heat conduction equation," Chap. 12 in *Optical-Thermal Response of Laser Irradiated Tissue*, A. J. Welch and M. J. C. van Gemert, Eds., pp. 385–409, Plenum Press, New York (1995).
19. V.-P. Gabel, R. Birngruber, and F. Hillenkamp, *Die Lichtabsorption am Augenhintergrund*, Gesellschaft für Strahlen-und-Univehforschung München, GSF Bericht A55 (1976).
20. A. J. Welch, E. H. Wissler, and L. A. Priebe, "Significance of blood flow in calculations of temperature in laser irradiated tissue," *IEEE Trans. Biomed. Eng.* **BME-27**, 164–166 (1980).